MECHANICAL PROPERTIES ANALYSIS AND RELIABILITY ASSESSMENT OF LAMINATED VENEER LUMBER (LVL) HAVING DIFFERENT PATTERNS OF ASSEMBLY

Bing Xue,[a,b] and Yingcheng Hu [a,*]

Laminated Veneer Lumber (LVL) panels made from poplar (*Populus ussuriensis* Kom.) and birch (*Betula platyphylla* Suk.) veneers were tested for mechanical properties. The effects of the assembly pattern on the modulus of elasticity (*MOE*) and modulus of rupture (*MOR*) of the LVL with vertical load testing were investigated. Three analytical methods were used: composite material mechanics, computer simulation, and static testing. The reliability of the different LVL assembly patterns was assessed using the method of Monte-Carlo. The results showed that the theoretical and ANSYS analysis results of the LVL *MOE* and *MOR* were very close to those of the static test results, and the largest proportional error was not greater than 5%. The veneer amount was the same, but the strength and reliability of the LVL made of birch veneers on the top and bottom was much more than the LVL made of poplar veneers. Good assembly patterns can improve the utility value of wood.

Keywords: Laminated veneer lumber (LVL); Mechanical properties; Assembly pattern; Reliability; Poplar; Birch

Contact information: a: Key Laboratory of Bio-based Material Science and Technology of Ministry of Education of China, College of Material Science and Engineering, Northeast Forestry University, Harbin, 150040, China; b: Heilongjiang Institute of Science and Technology, Harbin, 150027, China;
** Corresponding author: yingchenghu@163.com*

INTRODUCTION

Wood is a hard fibrous tissue found in many plants. It has many favorable properties such as its processing ability, physical and mechanical properties, and aesthetics, as well as being environmentally and health friendly. People have used wood in many ways for thousands of years, primarily as either a fuel or a construction material for making houses, tools, weapons, furniture, packages, artworks, and paper (Bodig and Jayne 1982; Liu 2004). In many countries wood is widely used as the main source of building material.

Laminated Veneer Lumber (LVL) is defined as "a general description for an assembly of veneers laminated with an adhesive in which the grain direction of the outer veneers and most other veneers are in the longitudinal direction" (ISO 18776:2008). An increasing demand for environmentally friendly materials has resulted in an increased interest in laminated veneer lumber, as it can be manufactured from sustainable wood resources. Because of the low energy requirement and the ability for high production, LVL has become more and more popular, deemed as a highly reliable engineered wood product (Hata et al. 2001). LVL proved its usefulness and efficiency in construction framing materials such as girders, beams, joists (either in association with OSB for I-beams, or alone to produce long structural beams), headers, lintels, and columns, as well as scaffold planks and panels. LVL can also be manufactured in different sizes to suit architectural and structural aims if necessary. The LVL manufacturing process is reported to generate products of several dimensions. LVL has advantages over solid wood in strength, predictability of performance, available sizes, dimensional consistency, dimensional stability, and treatability, along with a higher wood utilization rate (13% more than that of sawn wood) (Pirvu et al. 2000; Deam et al. 2008; Hayashi et al. 2005; Kurt 2010).

There are many factors that affect the mechanical properties of LVL, such as compression ratio, size, wood species, binding agent, veneer defects, growth ring characteristics, and density of LVL. Compression control has significant effects on the modulus of elasticity, modulus of rupture, specific gravity, and thickness swelling of poplar LVL (Zhang et al. 1994). The influence of the partial moments of inertia and binding agents (mixture of epoxy or phenol-formaldehyde resins with sawdust) on bending properties of the primary perforated spruce and lime elements have been investigated (Reinprecht and Joščăk 1994). The effect of size on bending strength has been experimentally determined for laminated veneer lumber. Size was found to have no effect on the modulus of elasticity or modulus of rigidity (Fonselius 1997). The compression strength and the static bending strength of both beech and spruce LVL panels were higher than those of the respective solid wood groups obtained from the same logs. The impact strength of LVL panels, unlike the static bending strength and compression strength, was lower than those of the solid samples, which were not steamed and aged (Semra et al. 2007). The effects of assembly pattern and loading direction on the bending strength and modulus of elasticity in laminated wood materials produced from 3 mm thick veneers of beech (*Fagus orientalis* L.) and lombardy poplar (*Populus nigra* L.) placed one on top of the other in various arrangements were examined. The bending strength and modulus of elasticity of the solid woods (measured both perpendicular and parallel to the glue line) were observed to be smaller than those of laminated woods made of the same species of wood (Erol et al. 2007). Veneer defect and growth ring pattern measurements, obtained via optical scanning, were hypothesized to improve LVL static tensile strength property predictions. Improved LVL static tensile strength predictions could be achieved by integrating ultrasonic and optical systems (DeVallance et al. 2011).

Reliability analysis and design traditionally consider an ultimate limit state (ULS) to define a failure event. For an ULS, the resistance or capability is represented by some measure of structural strength, representing a maximum value of the structural resistance. Failure is said to occur when the predicted load or demand exceeds the predicted strength. The dominant strength failure modes are usually some form of collapse or ductile overload. Proper inclusion of a strength prediction in a structural reliability context requires the characterisation and consideration of all possible strength uncertainties (Chen 2003).

In the present study, the structure reliability of LVL was investigated. Particular attention was paid to the effects of the assembly pattern on the mechanical properties of the LVL. Three analytical methods were used to analyze the LVL mechanical properties: composite material mechanics, finite element analysis software, and static testing.

EXPERIMENTAL

Wood Material

The rotary-cut veneers were made from panels composed of poplar (*Populus ussuriensis* Kom.) and birch (*Betula platyphylla* Suk.). The poplar and birch trees were harvested from Inner Mongolia. Round logs obtained from the trees were cut into stocks in rough sizes by taking into consideration final layer dimensions of 600 mm × 500 mm × 3.0 mm (length×width×thickness). A special emphasis was put on the selection of the wood material. Accordingly, non-deficient, proper, knotless, and normally grown (without zone line, reaction wood, decay, insect and fungal damages) wood materials were selected, making sure that the growth rings were perpendicular to the surface. The stocks were dried in a drying kiln until a moisture content of 7±1% was reached and were then stored in a natural environment. These stocks were later used to make 25 mm-thick ten-ply LVL in the laboratory.

Adhesive

The LVL panels were bonded with a commercial phenol-formaldehyde (PF) resin. The glue was spread at a rate of 150 g/m^2 onto a single surface of each layer. Glue was spread uniformly on the veneers by manually hand brushing. The glued layers were brought together immediately, one on the top of the other, and were kept this way for 30 min before being hot-pressed in a pressing machine for a duration of 40 min under a pressing temperature of 160 ºC and pressure of 1.5 MPa. The target thickness of LVL panels was 25 mm.

Assembly Patterns

There were ten-ply samples in nine different assembly patterns with 3.0 mm thickness veneers: (AAAAAAAAAA), (BBBBBBBBBB), (ABBBBBBBA), (AABBBBBBAA), (AAABBBBAAA), (AAAABBAAAA), (ABABAABABA), (BBAAAAAABB), and (BBBBAABBBB), with (A) representing birch wood and (B) representing poplar wood (Fig. 1).

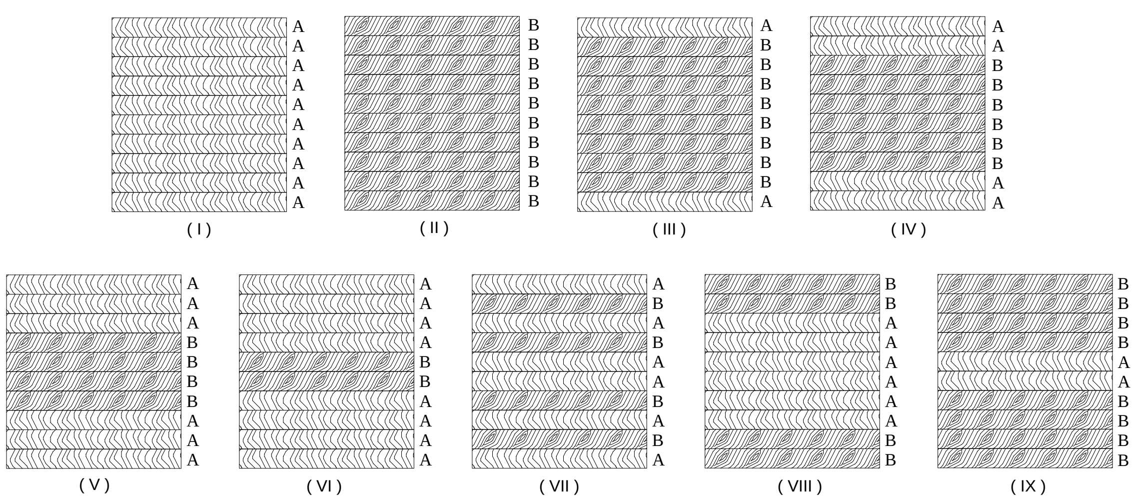

Fig. 1. Assembly patterns of the samples: (A) birch, (B) poplar

Preparation of Test Samples

Test samples with dimensions of 575×90×25 mm were obtained from the LVL panels and used for vertical load testing (Fig. 2). Ten specimens were produced for each assembly pattern. All test samples were placed in a climatization chamber (temperature of 20±2 ºC and relative humidity of 65±5%) until the weights of the samples remained constant, for the purpose of homogenization of moisture by volume before the experiments.

Experiment and Analysis

Theoretical analysis, computer simulation, and experimental research were conducted on the mechanical properties of the LVL.

Mechanical property analysis included stiffness and strength testing. For the stiffness evaluation, the analysis was divided into three main groups: micro-mechanics, macro-mechanics, and structural mechanics. For the application of composite materials, the macro-mechanics were analysed to grasp the actual performance of the composite structure.

The computer simulation used in this experiment is widely applied in all kinds of fields due to its ability to carry out large calculations. First, the mechanical properties of the LVL were simulated using the computer program to determine the feasibility of this method for the LVL, and reusing the reliability analysis function for the reliability assessment of the LVL.

The static bending tests were conducted on the specimens in accordance with the Japanese Agricultural Standard (JAS) of Structural Laminated Veneer Lumber.

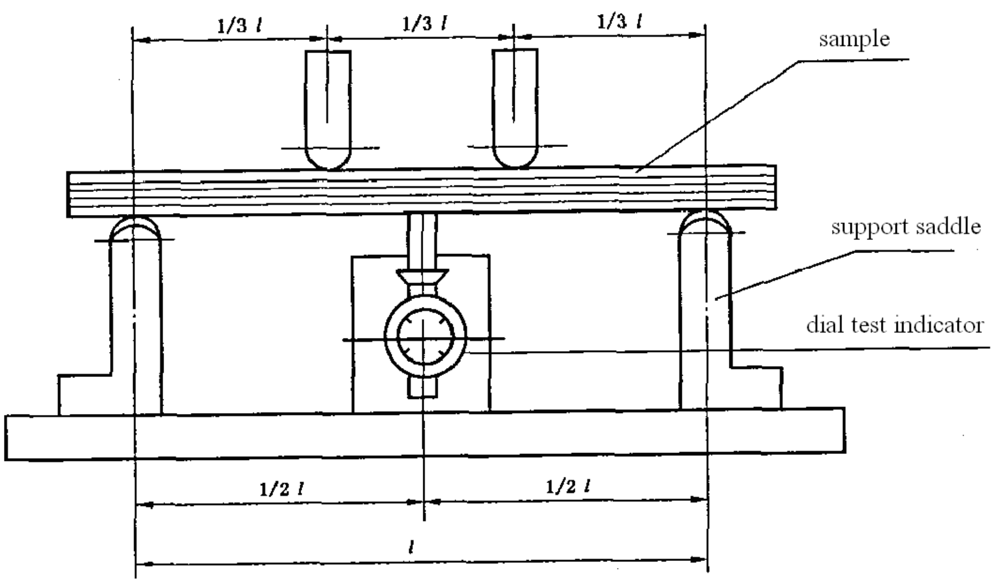

Fig. 2. Vertical load static test

The modulus of rupture is given by the equation:

$$MOR = Fl / bh^2 \quad (1)$$

where *MOR* is the modulus of rupture (MPa), *F* is the maximum load (N), *l* is the span in bending between the testing machine grips (mm), *b* is the cross sectional width in the bending test (mm), and *h* is the cross sectional thickness in the bending test (mm).

The modulus of elasticity is given by the equation:

$$MOE = 23\Delta Fl^3 / 108bh^3\Delta y \quad (2)$$

where *MOE* is the modulus of elasticity in bending perpendicular to the grain (GPa), ΔF is the increment of load on the regression line with a correlation coefficient of 0,99 or better (N), Δy is the increment of deformation corresponding to F_2 - F_1 (mm), and *l*, *b*, and, *h* are the same as in Equation (1).

Composite Material Mechanics Analysis

Rigidity analysis

In the theory of laminated beams in pure flexure, Young's modulus, or the extensional modulus, can be estimated using the rule of mixtures (Gibson 2011; Bodig and Jayne 1982)

$$E_x = E_1V_1 + E_2V_2 \quad (3)$$

where E_x is Young's modulus, or extensional modulus, of the laminated beam, E_1 is Young's modulus, or extensional modulus, of the first ply, E_2 is Young's modulus, or extensional modulus, of the second ply, V_1 is the volume fraction of the first ply, and V_2 is the volume fraction of the second ply.

The set of LVL panels was as a whole analyzed for mechanical properties. The thickness of the glue-lines was very thin, so the following presuppositions were enumerated for simplified analysis.

(1) The *MOE* of each veneer of a given wood species in the LVL panel was the same value;

(2) The adhesive spread in each glue-line was identical, and the glue was spread uniformity.

The deformation and breach of cell wall tissue texture was the provenance of the breach and deformation of the pure wood, as the cell wall is made of wood cellulose, lignin, and hemicellulose. The elasticity and strength of the panels were from the wood cellulose content. The cleavage strength of wood was attributed to hemicellulose. The elasticity and strength of wood was attributed to lignin (Liu 2004). The resistance to outside force was not changed after hot pressing because the amount of wood cellulose content in the LVL did not change. So the following expressions were found by introducing the theoretics of elasticity mechanics according as presuppositions,

$$E_L \times V_L = E_C \times V_C \quad (4)$$

where E_L is the longitudinal *MOE* of LVL after hot pressing, V_L is the volume of the LVL after hot pressing, E_C is the longitudinal *MOE* of clear wood before hot pressing, and V_C is the volume of clear wood before hot pressing.

$$E_C = E_b V_b + E_p V_p \quad (5)$$

In Eq. 5, E_b is the longitudinal *MOE* of birch clear wood, V_b is volume fraction of birch veneers, E_p is the longitudinal *MOE* of poplar clear wood, and V_p is volume fraction of poplar veneers.

The theoretical *MOE* of the LVL panels can be obtained from Eqs. (4) and (5), and E_b and E_p can be obtained from the static bending tests.

Strength analysis

Macromechanical failure theories in composite materials include the maximum stress theory, maximum strain theory, Tsai-Hill theory (deviatoric strain energy theory), and Tsai-Wu theory (interactive tensor polynomial theory).

The maximum stress criterion states that failure occurs when at least one stress component along the principal material axes exceeds the corresponding strength in that direction. It can be expressed as,

$$\text{Tensile stresses: } \sigma_1 \geq F_{1t} \text{ (Fiber break) or } \sigma_2 \geq F_{2t} \text{ (Matrix crack),} \quad (6)$$

$$\text{Compressive stresses: } \sigma_1 \leq F_{1c} \text{ (Fiber crushing) or } \sigma_2 \leq F_{2c} \text{ (Matrix yielding),} \quad (7)$$

where σ_1 and σ_2 are the longitudinal and transverse principal stresses, and F_1 and F_2 are the longitudinal and transverse allowable tensile (*t*) or compressive (*c*) stresses.

The maximum strain criterion states that failure occurs when at least one of the strain components along the principal material axes exceeds the ultimate strain in that direction. It can be expressed as,

$$\text{Tensile stresses: } \varepsilon_1 \geq \varepsilon_{1t}^u \text{ (Fiber break) or } \varepsilon_2 \geq \varepsilon_{2t}^u \text{ (Matrix crack),} \quad (8)$$

$$\text{Compressive stresses: } \varepsilon_1 \leq \varepsilon_{1c}^u \text{ (Fiber crushing) or } \varepsilon_2 \leq \varepsilon_{2c}^u \text{ (Matrix yielding),} \quad (9)$$

where ε_1 and ε_2 are the longitudinal and transverse principal strains and ε_1^u and ε_2^u are the longitudinal and transverse allowable tensile (*t*) or compressive (*c*) strains.

The Tsai-Hill theory originated from an extension of the Von Mises criterion for ductile anisotropic materials. Azzi-Tsai extended this equation to include anisotropic fiber reinforced composites. The Tsai-Wu theory is a simplification of the Gol'denblat and the Kapnov generalized failure theories for anisotropic materials (Gibson 2011). Both apply to material strength analysis in a complex stress state. Maximum stress or strain criterion can satisfy the requirements of strength analysis in this study.

Computer Simulation

ANSYS offers a comprehensive range of engineering simulation solution sets, providing access to any virtual field of engineering simulation that a design process requires. This finite element analysis program was applied to simulate the mechanical properties of the LVL in this study. Structural mechanical solutions from ANSYS provide the ability to simulate every structural aspect of a product. In order to examine the distribution of internal stress of each ply of the LVL, simulating by the PLANE82 element, the simulation analysis was executed using the same acting point of force as a static experiment.

Reliability Analysis

As a generalization in structural design, the variables representing the load effects the resistance properties of the structure and cannot be known completely; therefore, they must be described as random variables, which have a mean and an assumed underlying probability distribution. A given design situation can be described mathematically by a function of the basic random variables in the form,

$$g(\mathrm{X}) = g(\mathrm{X}_1, \mathrm{X}_2, \ldots, \mathrm{X}_n) \qquad (10)$$

where $X = (\mathrm{X}_1, \mathrm{X}_2, \ldots \mathrm{X}_n)$ is the vector of these basic random variables. By convention, the limit state function $g(\mathrm{X})$ is formulated such that $g(\mathrm{X})<0$ when the structure does not perform as intended (known as "failure").

In this study, the generalized reliability level was assessed by the first order second moment method, the second order second moment method, and the stochastic finite element method, etc. (Gong and Wei 2007).

The Monte-Carlo method is a stochastic finite element method. Monte-Carlo simulations have the major advantage of producing accurate solutions, which can be obtained for any problem whose deterministic solution is known, since it statistically converges to the correct solution provided that a large number of simulations are employed. The basic principles of direct Monte-Carlo simulations are used to generate a sampling of the input parameters in accordance with their probability distributions and correlations. For each input sample, a deterministic finite element analysis is carried out, giving an output sample. Finally, a response sampling is obtained, from which the mean and the standard deviation of the response can be derived.

The estimator of the response $\overline{y}$ is defined by

$$\overline{y} = \frac{1}{n}\sum_{i=1}^{n} y^{(i)} \qquad (11)$$

where n is the number of samples and $y^{(i)}$ is the response corresponding to the i*th* input sample (Schenk and Schuëller 2005). The estimator is a random variable whose mean and variance are given by

$$E[\overline{y}] = \mu_y \qquad (12)$$

and

$$Var(\overline{y}) = E[(\overline{y} - E[\overline{y}])^2] = \frac{\sigma_y^2}{n} \qquad (13)$$

where $\mu_y = E[y]$ and $\sigma_y^2 = E[(y-\mu_y)^2]$ denote the unknown mean and variance of the response, respectively. Tchebychev's inequality provides a basis for error assessment, i.e.,

$$P(\left|\bar{y}-\mu_y\right| < \varepsilon) \geq 1 - \frac{1}{\varepsilon^2}\frac{\sigma_y^2}{n} \tag{14}$$

where ε denotes a tolerance. A confidence level 1-δ can be defined where $\delta = \frac{1}{\varepsilon^2}\frac{\sigma_y^2}{n}$. According to the central limit theorem, the distribution of $\bar{y}$ is normal and the confidence interval corresponding to the confidence level 1-δ is,

$$\mu_{y,1-\delta} = \left[\bar{y} - \Phi^{-1}(1-\delta/2)\frac{\sigma_y^2}{\sqrt{n}}, \bar{y} + \Phi^{-1}(1-\delta/2)\frac{\delta_y^2}{\sqrt{n}}\right] \tag{15}$$

where Φ is the normal cumulative distribution function.

Derivation of serviceability limit state function

A serviceability limit state for LVL systems can be defined in terms of a limiting maximum mid-span deflection, typically expressed as a fraction of the span. The span cannot be arbitrarily chosen, since the design of the LVL system must be in accordance with existing code provisions. The mid-span deflection calculation of flexural members is not more than,

$$Z_n = l/360 \tag{16}$$

where Z_n is the allowable deflection and l is the span length.

$$Z_u \leq \varphi Z_n \tag{17}$$

where Z_u is the deflection due to the factored nominal loads and φ is a serviceability resistance factor.

The deflection Z_u in this study's static bending tests should be expressed as,

$$Z_u = 23Fl^3/108E_n bh^3 \tag{18}$$

where F is the test load, E_n is the nominal elastic modulus, b is the cross sectional width in a bending test specimen, and h is the cross sectional thickness in a bending test specimen.

To ensure conservative results in the reliability analyses, the upper limit of the span length was used. After establishing the relationship between the span and the size, the serviceability limit state function is written as,

$$g(\mathrm{X}) = \frac{l}{360} - \max(\delta_t) \tag{19}$$

where δ_t is the maximum deflection occurring during the reference period due to the characteristic of the random variable.

Derivation of Strength Limit State Function

A strength checking equation for a LVL system may be written in a form that includes a system factor,

$$\lambda\gamma Z_n \geq Z_u \tag{20}$$

where Z_n is the nominal strength (i.e. the flexural moment capacity), Z_u is the required strength (i.e. the moment created by the factored loads), λ is a factor that accounts for duration of-load effects, and γ is a strength resistance factor. The Z_n can be regarded as the theoretical and experimental *MOR* of the LVL in this study.

Individual members in the system were deemed to have failed the strength limit state when either the flexural stresses exceeded the *MOR* or the accumulated damage reached the limit state defined by,

$$g(\mathrm{X}) = 1 - \sum_i \alpha_i \tag{21}$$

where α_i is the damage increments produced by each of the random variable pulses.

RESULTS AND DISCUSSION

Mechanics Analysis

The *MOR* (σ_i) and *MOE* (E_C) of poplar and birch clear wood before hot pressing were obtained by a bending statics test. Ten specimens were produced for each wood, and the average values are provided in Table 1, along with the standard deviations (STD) of each wood test. The theoretical *MOR* and *MOE* of each LVL assembly pattern after hot pressing could be determined by substituting σ_i into Eqs. (6) and (7) or by substituting E_C into Eqs. (4) and (5). All the theoretical *MOR* and *MOE* of each assembly pattern after hot pressing are provided in Tables 3 and 4 in order to facilitate the comparison of all analysis results.

Table 1. The *MOR* and *MOE* of Clear Wood

Species	*MOR* (MPa)	STD of *MOR* (MPa)	*MOE* (GPa)	STD of *MOE* (GPa)
Birch	154.613	8.986	16.882	0.963
Poplar	129.449	13.226	15.605	0.975

ANSYS Analysis

The mechanical properties of different LVL assembly patterns were simulated using the finite element analysis program ANSYS to examine the practicability of finite element analysis on LVL. With a vertical loading of 1 N, the stress distributions on the vertical longitudinal section of the LVL test specimens for assembly patterns (I), (II), and (III) are provided in Fig. 3. The changes in stress distribution gradient were a pretty clear distinction among those various LVL assembly patterns; these results were consistent with the composite material mechanical analysis results and therefore the maximum plus-minus stress on each assembly pattern were different.

In order to show a clearer stress distribution of each LVL specimen, assembly patterns (I) and (VII) were chosen, and the stress distribution along the thickness direction of the mid-span section for the two assembly patterns are shown in Figs. 4 and 5, and the maximum stress for each assembly pattern are shown in Table 2.

The analysis results of *MOR* and *MOE* were obtained by ANSYS, and are provided in Tables 3 and 4 in order to facilitate the comparison of all analysis results.

Table 2. The Maximum Stress in Each Assembly Pattern

Assembly pattern	I	II	III	IV	V
Maximum stress (Pa)	1680.000	1680.000	1926.605	1775.898	1707.317
Assembly pattern	VI	VII	VIII	IX	
Maximum stress (Pa)	1683.366	1842.105	1567.164	1675.531	

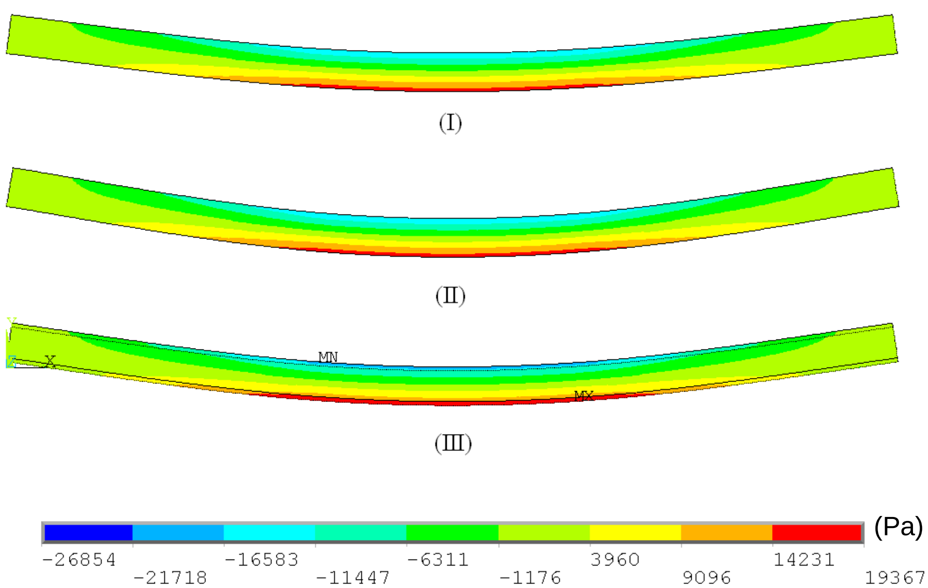

Fig. 3. The stress distribution on vertical longitudinal section of assembly patterns (I), (II), and (III)

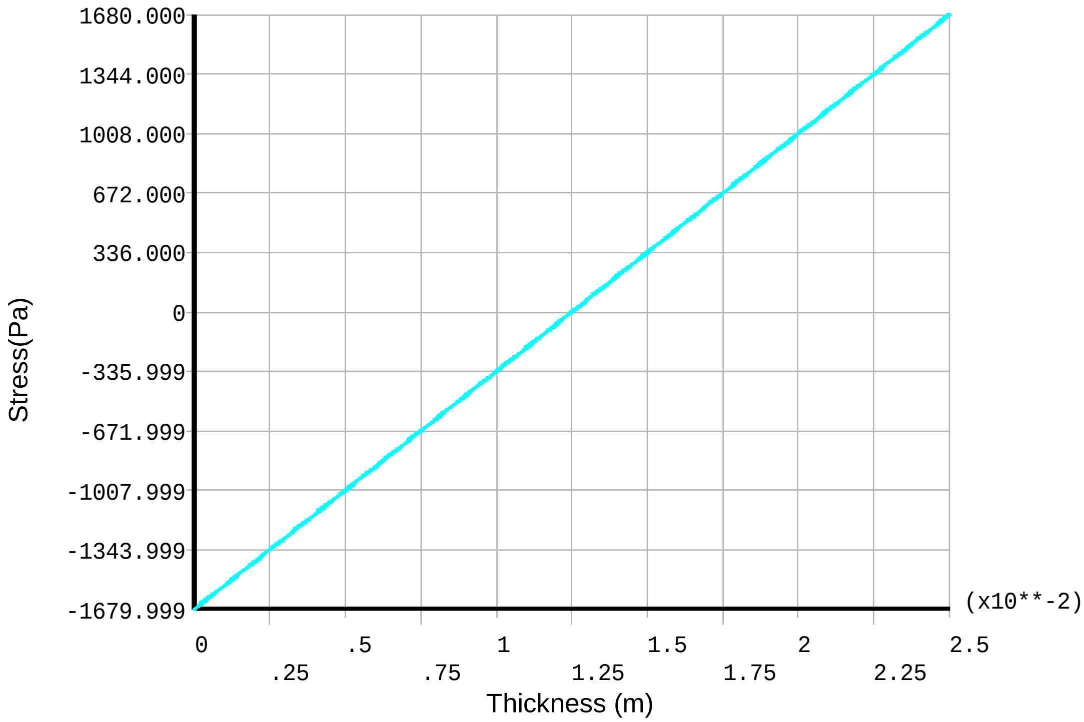

Fig. 4. The stress distribution along the thickness direction of the mid-span section of assembly pattern (I)

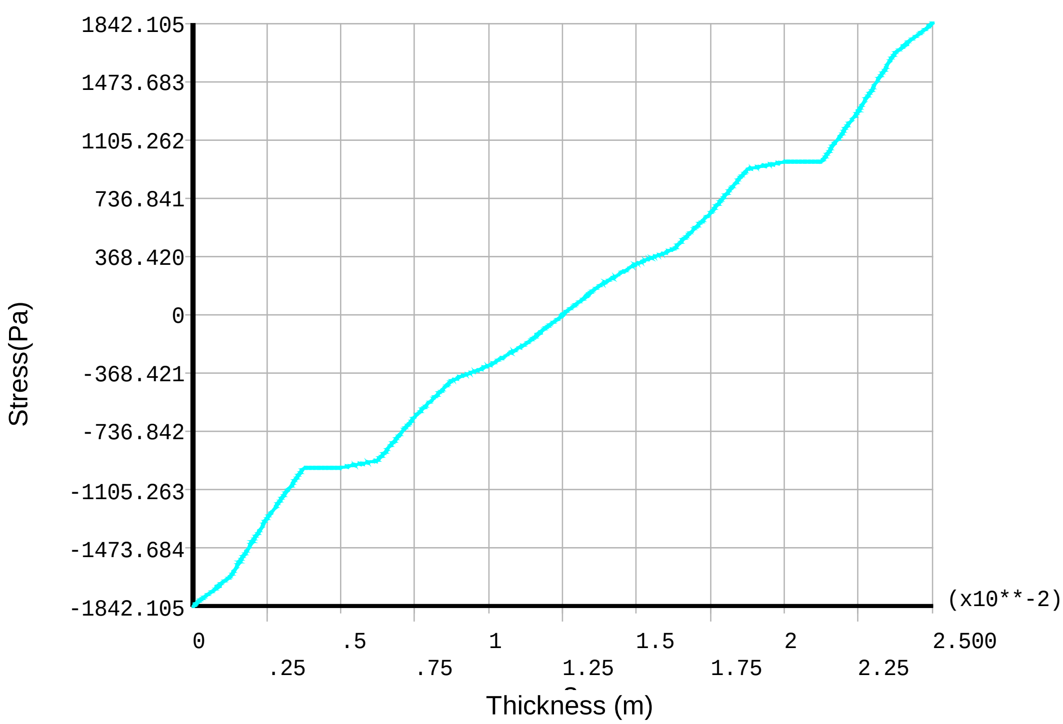

Fig. 5. The stress distribution along the thickness direction of the mid-span section of assembly pattern (VII)

As shown in Figs. 4 and 5, the ply direction path mid-span stress distribution curves of assembly patterns (I) and (II) were straight lines, while those of other patterns not provided and assembly pattern (VII) were curves. Obviously, the different wood species of each layer caused the change in stress distribution: the form of the stress distribution had become more complicated, the slope had an obvious change in the place of the two different wood species junction, and the curve line slope of assembly pattern (VII) had the greatest change (so it was chosen to show stress change). The main reason for the change is that birch (A) and poplar (B) have different *MOE*. LVL assembly patterns (I) and (II) were nearly uniform in rigidity, because of the effective bonding between (A) and (B), which affected deformation coordination, so other assembly patterns were not. Nevertheless, assembly pattern (VII) was assembled with an alternative distribution of (A) and (B) and its *MOE* varied for each ply.

As shown in Table 2, the maximum stress was associated with assembly pattern (III), and the minimum with assembly pattern (VIII). The main reason of the aforementioned results was that the *MOE* of birch (A) is greater than that of poplar (B), meaning a greater resistance to deformation for (A), so the existence of deformation coordination made the birch veneers a major contributor; the margin plate was (A) in LVL assembly pattern (III) and the margin plate was (B) in LVL assembly pattern (VIII).

The result of ANSYS analysis was consistent with the composite material mechanics analysis, so the ANSYS software can be applied to LVL mechanical analysis.

Static Test

The *MOE* and *MOR* of each LVL assembly pattern were obtained by a bending statics test, and the average values are provided in Tables 3 and 4. The failure mode of each LVL specimen was veneer breakdown during the flexural testing, the phenomemon of adhesive debonding did not occur, all test results were available.

Table 3. The Three Results of *MOE* of Each Assembly Pattern (GPa)

Assembly pattern	Theoretical results (MOE_1)	ANSYS analysis results (MOE_2)	Test results (*MOE*)	(MOE_1-*MOE*)/*MOE*	(MOE_2-*MOE*)/*MOE*
I	20.258	20.166	20.337	-0.39%	-0.84%
II	18.726	18.536	18.691	0.19%	-0.83%
III	19.020	19.326	19.254	-1.22%	0.38%
IV	19.350	19.812	19.036	1.65%	4.07%
V	19.679	20.053	19.687	-0.04%	1.86%
VI	20.008	20.146	20.100	-0.46%	0.23%
VII	19.679	19.595	20.055	-1.87%	-2.29%
VIII	19.679	18.891	19.213	2.43%	-1.67%
IX	19.020	18.554	19.365	-1.78%	-4.19%

As shown in Table 3, MOE_1 or MOE_2 of each assembly pattern was very close to the *MOE* results, with each proportional error absolute value not greater than 2.43% or 4.19% with the confidence coefficient being greater than the general confidence limit of 95%. So Eqs. 3 to 5 and ANSYS simulation analysis were appropriate for the rigidity solution of LVL mechanical properties, which can be applied to the reliability analysis of LVL in serviceability limit states.

Table 4. The Three *MOR* Results of Each Assembly Pattern (MPa)

Assembly pattern	Theoretical results (MOR_1)	ANSYS analysis results (MOR_2)	Test results (MOR)	(MOR_1-MOR)/MOR	(MOR_2-MOR)/MOR
I	185.536	185.536	185.835	-0.16%	-0.16%
II	155.339	155.339	153.298	1.33%	1.33%
III	165.396	161.787	168.835	-2.04%	-4.17%
IV	161.493	175.517	168.189	-3.98%	4.36%
V	172.591	182.567	178.194	-3.14%	2.45%
VI	177.689	185.165	178.964	-0.71%	3.46%
VII	177.587	169.209	177.935	-0.20%	-4.90%
VIII	161.602	166.523	164.158	-1.56%	1.44%
IX	159.389	155.753	162.962	-2.19%	-4.42%

As shown in Table 4, MOR_1 or MOR_2 of each assembly pattern was very close to the test results *MOR*, with each proportional error absolute value not greater than 3.98% or 4.90%, with a confidence coefficient greater than 95%. So obviously, Eqs. 6 and 9 and ANSYS simulation analysis were appropriate for the strength solution of LVL mechanical properties, and they can be applied to the reliability analysis of LVL in strength limit states.

There was the same amount of poplar and birch veneers in assembly patterns (III) and (IX). Pattern (V) had the same amount as (VII) and (VIII), but their *MOR* were much different; the *MOR* of assembly pattern (III) was more than that of assembly pattern (IX), and the *MOR* of assembly pattern (V) was close to that of (VII) and more than that of (VIII). The main reason is as follows: although the veneer dosages were the same, the internal stress was a symmetric triangular distribution along the vertical cross section, the stress was zero on the plane of symmetry, lower elastic layers receiving less stress (Serrano et al. 1996), so the strength of the LVL with high strength birch veneers on the top and bottom was much more than the strength of the LVL with low strength poplar veneers on the top and bottom. So a good assembly pattern can improve the utility value of wood and get a better ratio of strength to price.

Reliability Analysis

The reliability analysis of LVL was divided into two parts. The first was serviceability limit state and the second was strength limit state. The random variables included the *MOR* and *MOE* of poplar and birch clear wood, the width and thickness of LVL specimens, and the different load conditions. The existing random variables from the test are provided in Table 5. The load conditions referenced the related standard, as the applications that confine the two kinds limit states are different. Two load conditions were chosen; the first condition was used for the reliability analysis of the serviceability limit state, and the other was used to for the reliability analysis of the strength limit state.

The relevant data was input to the ANSYS, using the reliability analysis function. The reliability of each LVL was obtained and provided in Table 6, with P_r representing the reliability by the serviceability limit state and P_r' representing the reliability by the strength limit state.

Table 5. The Random Variables of Test Data

Assembly pattern	The average of width (mm)	STD of width data	The average of thickness (mm)	STD of thickness data	STD of MOE data	STD of MOR data
I	90.713	0.145	24.612	0.116	0.920	8.593
II	90.543	0.301	24.408	0.192	0.913	13.249
III	90.495	0.443	24.446	0.131	0.554	4.173
IV	90.594	0.407	24.150	0.095	0.724	12.821
V	90.420	0.441	24.137	0.073	0.714	8.736
VI	90.498	0.321	24.478	0.143	0.651	9.922
VII	89.856	0.096	24.184	0.173	1.269	13.804
VIII	89.814	0.164	24.289	0.151	0.448	8.761
IX	89.919	0.125	24.150	0.128	0.720	8.571

Table 6. The Reliability of Different Assembly Patterns LVL

Assembly pattern	I	II	III	IV	V	VI	VII	VIII	IX
P_r	1.0000	0.9287	1.0000	0.9948	0.9999	0.9998	0.9988	0.9988	0.9985
P_r'	0.9797	0.9621	0.9702	0.9672	0.9744	0.9783	0.9762	0.9699	0.9710

As shown in Table 6, the maximum reliability achieved was with assembly patterns (I) and (III) in the serviceability limit state and (I) in the strength limit state. The minimum reliability was with assembly pattern (II) in the serviceability limit state, and the strength limit state was the same for all patterns. As described above, there were equal amounts of poplar and birch veneers in assembly patterns (III) and (IX); (V) was the same as (VII) and (VIII), but their mechanical properties were much different. The reliability was also different under the same load conditions; the reliability of assembly pattern (III) was more than that of assembly pattern (IX), and the reliability of assembly pattern (V) was close to that of (VII) and (VIII) in the serviceability limit state, but the reliability of assembly patterns (V) and (VII) were more than that of (VIII) in the strength limit state. The main reason for this is as follows: the same veneer dosage of LVL had similar *MOE* and different *MOR*, the central interlayer had less of an effect on the strength and strength reliability of LVL.

CONCLUSIONS

1. The *MOE* results of theoretical analysis of each LVL assembly pattern were very close to the test results. The confidence coefficients were above the general confidence limit at 95%. Thus, Eqs. 4 and 5 can be considered as appropriate for the rigidity solution of LVL mechanical properties.
2. The *MOR* results of the theoretical analysis of each LVL assembly pattern were very close to the test results. The maximum stress and maximum strain criterion were found to be appropriate for the strength solution of LVL mechanical properties.

3. Similarly, the ANSYS simulation analyses were appropriate for the LVL mechanical property analysis.
4. Although the veneer dosages were the same, the strength of LVL with birch veneers on the top and bottom were much greater than the strengths of LVL with poplar veneers on the top and bottom. A good assembly pattern can improve the utility value of wood and provide a better strength-to-price ratio.
5. When the veneer dosages were the same, the *MOE* of each LVL assembly pattern was very close, and the serviceability limit state reliabilities were close as well. The strength limit state reliability was different, however, with the reliability of LVL with birch veneers on the outer surface being greater.
6. These results pertain to LVL that is defect-free and may not hold true if defects and varied grain deviations are present in the veneer that makes up typical LVL.

ACKNOWLEDGMENTS

This project was supported by the National Natural Science Foundation of China (31170516), the Program for A Foundation for the Author of National Excellent Doctoral Dissertation (200764), the Fundamental Research Funds for the Central Universities (DL09DB02), and the Scientific Research Fund of Heilongjiang Provincial Education Department (NO: 12511488).

REFERENCES CITED

Biblis, E. J. (1996). "Comparison of flexural and shear properties of southern pine LVL and lumber from young plantation and natural stands," *Ann. Sci. For.* 53(6), 1167-1175.

Bodig, J., and Jayne, B. A. (1982). *Mechanics of Wood and Wood Composites*, Van Nostrand and Reinhold, New York.

Chen, N. Z., Sun, H. H., and Soares, C. G. (2003). "Reliability analysis of a ship hull in composite material," *Composite Structures* 62(1), 59-66.

Deam, B. L., Fragiacomo, M., and Buchanan, A. H. (2008). "Connections for composite concrete slab and LVL flooring systems," *Materials and Structures* 41(3), 495-507.

DeVallance, D. B., Funck, J. W., and Reeb, J. E. (2011). "Evaluation of laminated veneer lumber tensile strength using optical scanning and combined optical-ultrasonic techniques," *Wood Fiber Sci.* 43(2), 169-179.

Erol, B., Murat, K., Abdullah, C. I., and Ozan, U. (2007). "The effects of assemble pattern and loading direction on bending strength and modulus of elasticity in laminated veneer lumber (LVL) obtained from beech (*Fagus orientalis* L.) and lombardy poplar (*Populus nigra* L.)," *Construction and Building Materials* 21(8), 1720-1725.

Fonselius, M. (1997). "Effect of size on the bending strength of laminated veneer lumber," *Wood Science and Technology* 31(6), 399-413.

Gibson, R. F. (2011). *Principles of Composite Material Mechanics*, CRC Press, Boca Raton.
Gong, J. X., and Wei, W. W. (2007). *Engineering Structure Reliability Design Principle*, China Machine Press, Beijing (in Chinese).
Harding, O. V., Van, Wyk. J. L., and Orange, R. P. (1998). "Influence of three processing strategies on stiffness and dimensional stability of radiata pine structural lumber," *Forest Prod. J.* 48(5), 57-62.
Hata, T., Umemura, K., Yamauchi, H., Nakayama, A., Kawai, S., and Sasaki, H. (2001). "Design and pilot production of a "spiral-winder" for the manufacture of cylindrical laminated veneer lumber," *J. Wood Sci.* 47(2), 115-123.
Hayashi, T., Miyatake, A., and Harada, M. (2002). "Outdoor exposure tests of structural laminated veneer lumber (I): evaluation of the physical properties after six years," *J. Wood Sci.* 48(1), 69-74.
International Standard ISO 18776 (2008). *Laminated Veneer Lumber (LVL) — Specifications*, Switzerland.
Kurt, R. (2010). "Suitability of three hybrid poplar clones for laminated veneer lumber manufacturing using melamine urea formaldehyde adhesive," *BioResources* (http://www.bioresources.com) 5(3), 1868-1878.
Liu, Y. X. (2004). *Woodiness Resource Materials Science*, China Forestry publishers, Beijing (in Chinese).
Nzokou, P., Zyskowski, J., Boury, S., and Kamdem, D. P. (2005). "Natural decay resistance of LVL made of veneers from durable and non-durable wood species," *Holz als Roh- und Werkstoff* 63(3), 173-178.
Pirvu, C., Yoshida, H., and Taki, K. (2000) "Development of LVL frame structures using glued metal plate joints. II. Strength properties and failure behavior under lateral loading," *J. Wood Sci*. 46(3), 193-201.
Reinprecht, L., and Joščăk, P. (1994). "Reinforcement of model-damaged wooden elements. Part 1. Local perforation of wooden elements and their gap-filling treatment" *Drevársky Výskum* 39(4), 1-21.
Schenk, C. A., and Schuëller, G. I. (2005). *Uncertainty Assessment of Large Finite Element Systems*, Springer, Austria.
Semra, Ç., Gürsel, Ç., and Ismail, A. (2007). "Effects of logs steaming, veneer drying and aging on the mechanical properties of laminated veneer lumber (LVL)," *Building and Environment* 42(1), 93-98.
Serrano, E., Gustafsson, P., and Larsen, H. (1996). "Lamination effect and finger joints analysed by fracture mechanics," *Proc. Intl. Wood Eng. Conf.* 4, 295-302.
Shupe, T. F., Hse, C. Y., Groom, L. H., and Choong, E. T. (1997). "Effect of silvicultural practice and veneer grade lay-up on some mechanical properties of loblolly pine LVL," *Forest Prod J* 47(9), 63-69.
Zhang, H. J., Chui, Y. H., and Schneider, M. H. (1994). "Compression control and its significance in the manufacture and effects on properties of poplar LVL," *Wood Science and Technology* 28(4), 285-290.

Article submitted: December 1, 2011; Peer review completed: January 15, 2012; Revised version received and accepted: February 11, 2012; Published: February 14, 2012.